Contents

Chapter 18

Convection

Version 1218.2.K, 9 June 2013 *Please send comments, suggestions, and errata via email to kip@caltech.edu or on paper to Kip Thorne, 350-17 Caltech, Pasadena CA 91125*

Box 18.1
Reader's Guide

- This chapter relies heavily on Chap. 13.
- No subsequent chapters rely substantially on this one.

18.1 Overview

In Chaps. 13 and 14, we demonstrated that viscosity can exert a major influence on subsonic fluid flows. When the viscosity ν is large and the Reynolds' number $\mathrm{Re} = LV/\nu$ is low, viscous stresses transport momentum directly, and the fluid's behavior can be characterized by saying that the vorticity ($\boldsymbol{\omega} = \boldsymbol{\nabla} \times \mathbf{v}$) *diffuses* through the fluid [cf. Eq. (14.3)]. As the Reynolds' number increases, the *advection* of the vorticity becomes more important. In the limit of large Reynolds' number, we think of the vortex lines as being *frozen* into the flow. However, as we learned in Chap. 15, this insight is only qualitatively helpful because high Reynolds' number flows are invariably turbulent. Large, irregular, turbulent eddies transport shear stress very efficiently. This is particularly in evidence in turbulent boundary layers.

When viewed microscopically, heat conduction is a similar transport process to viscosity, and it is responsible for analogous physical effects. If a viscous fluid has high viscosity, then vorticity diffuses through it rapidly; simularly, if a fluid has high thermal conductivity, then heat diffuses through it rapidly. In the other extreme, when viscosity is low (i.e., when the Reynolds number is high), instabilities produce turbulence, which transports vorticity far more rapidly than diffusion could possibly do. Analogously, in heated fluids with low conductivity, the local accumulation of heat drives the fluid into convective motion, and

the heat is transported much more efficiently by this motion than thermal diffusion could possibly do. As the convective heat transport increases, the fluid motion becomes more vigorous and, if the viscosity is sufficiently low, the thermally driven flow can also become turbulent. These effects are very much in evidence near solid boundaries, where thermal boundary layers can be formed, analogous to viscous boundary layers.

In addition to thermal effects that resemble the effects of viscosity, there are also unique thermal effects—particularly the novel and subtle combined effects of gravity and heat. Heat, unlike vorticity, causes a fluid to expand and thus, in the presence of gravity, to become buoyant; and this buoyancy can drive thermal circulation or *free convection* in an otherwise stationary fluid. (Free convection should be distinguished from *forced convection* in which heat is carried passively in a flow driven by externally imposed pressure gradients, for example when you blow on hot food to cool it, or stir soup over a hot stove.)

The transport of heat is a fundamental characteristic of many flows. It dictates the form of global weather patterns and ocean currents. It is also of great technological importance and is studied in detail, for example, in the cooling of nuclear reactors and the design of automobile engines. From a more fundamental perspective, as we have already discussed, the analysis and experimental studies of convection have led to major insights into the route to chaos (Sec. 15.6).

In this chapter, we shall describe some flows where thermal effects are predominant. We shall begin in Sec. 18.2 by writing down and then simplifying the equations of fluid mechanics with heat conduction. Then in Sec. 18.3 we shall discuss the *Boussinesq approximation*, which is appropriate for modest scale flows where buoyancy is important. This will allow us in Sec. 18.4 to derive the conditions under which convection is initiated. Unfortunately, this Boussinesq approximation sometimes breaks down. In particular, as we shall discuss in Sec. 18.5, it is inappropriate for convection in stars and planets, where circulation takes place over several gravitational scale heights. Here, we shall have to use alternative, more heuristic arguments to derive the relevant criterion for convective instability, known as the *Schwarzschild criterion*, and to quantify the associated heat flux. We shall apply this theory to the solar convection zone.

Finally, in Sec. 18.6 we shall return to simple buoyancy-driven convection in a stratified fluid to consider *double diffusion*, a quite general type of instability which can arise when the diffusion of two physical quantities (in our case heat and the concentration of salt) render a fluid unstable despite the fact that the fluid would be stably stratified if there were only concentration gradients of one of these quantities.

In previous fluid chapters, we recommended movies that give physical insight into the phenomena studied. Unfortunately, we do not know of any suitable movies about convection.

18.2 T2 Diffusive Heat Conduction — Cooling a Nuclear Reactor; Thermal Boundary Layers

So long as the mean free path of heat-carrying particles is small compared to the fluid's inhomogeneity lengthscales (as is almost always the case), and the fractional temperature change in one mean free path is small (as is also almost always true), the energy flux due to

heat flow takes the thermal-diffusion form

$$\mathbf{F}_{\rm cond} = -\kappa \boldsymbol{\nabla} T \ ; \tag{18.1}$$

see Secs. 3.7 and 13.7.4. Here κ is the thermal conductivity.

For a viscous, heat-conducting fluid flowing in an external gravitational field, the most general governing equations are the fundamental thermodynamic potential $u(\rho, s)$; the first law of thermodynamics, Eq. (2) or (3) of Box 13.2; the law of mass conservation (13.29) or (13.31); the Navier-Stokes equation (13.69); and the law of dissipative entropy production (13.75):

$$\begin{aligned}
u &= u(\rho, s) \ , && \text{(18.2a)}\\
\frac{du}{dt} &= T\frac{ds}{dt} - P\frac{d(1/\rho)}{dt} \ , && \text{(18.2b)}\\
\frac{d\rho}{dt} &= -\rho \boldsymbol{\nabla}\cdot\mathbf{v} \ , && \text{(18.2c)}\\
\rho\frac{d\mathbf{v}}{dt} &= -\boldsymbol{\nabla} P + \rho\boldsymbol{g} + \boldsymbol{\nabla}(\zeta\theta) + 2\nabla\cdot(\eta\boldsymbol{\sigma}) \ , && \text{(18.2d)}\\
T\left[\rho\left(\frac{ds}{dt}\right) + \boldsymbol{\nabla}\cdot\left(\frac{-\kappa\boldsymbol{\nabla}T}{T}\right)\right] &= \zeta\theta^2 + 2\eta\boldsymbol{\sigma}:\boldsymbol{\sigma} \ + \frac{\kappa}{T}(\boldsymbol{\nabla}T)^2 \ . && \text{(18.2e)}
\end{aligned}$$

These are four scalar equations and one vector equation for four scalar and one vector variables: the density ρ, internal energy per unit mass u, entropy per unit mass s, pressure P, and velocity $\mathbf{v}$. The thermal conductivity κ and coefficients of shear and bulk viscosity ζ and $\eta = \rho\nu$ are presumed to be functions of ρ and s (or equally well, ρ and T).

This set of equations is far too complicated to solve, except via massive numerical simulations, unless some strong simplifications are imposed. We therefore introduce approximations. *Our first approximation* (already implicit in the above equations) is that *the thermal conductivity κ is constant, as are the coefficients of viscosity;* for most real applications this is close to true, and no significant physical effects are missed by assuming it. *Our second approximation,* which does limit somewhat the type of problem we can address, is that *the fluid motions are very slow*—slow enough that, not only can the flow be regarded as incompressible ($\theta = \boldsymbol{\nabla}\cdot\mathbf{v} = 0$), but the squares of the shear $\boldsymbol{\sigma}$ and expansion θ (which are quadratic in the fluid speed) are negligibly small, and we thus can ignore viscous dissipation. These approximations bring the the last three of the fluid evolution equations (18.2) into the simplified form

$$\begin{aligned}
\boldsymbol{\nabla}\cdot\mathbf{v} &\simeq 0 \ , \quad d\rho/dt \simeq 0 \ , && \text{(18.3a)}\\
\frac{d\mathbf{v}}{dt} &= -\frac{\boldsymbol{\nabla} P}{\rho} + \boldsymbol{g} + \nu\nabla^2\mathbf{v} \ , && \text{(18.3b)}\\
\rho T\frac{ds}{dt} &= \kappa\nabla^2 T. && \text{(18.3c)}
\end{aligned}$$

[Our reasons for using "$\simeq$" in Eqs. (18.3a) will become clear in Sec. 18.3 below, in connection with buoyancy.] Note that Eq. (18.3b) is the standard form of the Navier Stokes equation for

incompressible flows, which we have used extensively in the past several chapters. Equation (18.3c) is an elementary law of energy conservation; it says that the rate of increase of entropy density moving with the fluid is equal to minus the divergence of the conductive energy flux $\mathbf{F}_{\rm heat} = -\kappa \boldsymbol{\nabla} T$.

We can convert the entropy evolution equation (18.3c) into an evolution equation for temperature by expressing the changes ds/dt of entropy per baryon in terms of changes dT/dt of temperature. The usual way to do this is to note that Tds (the amount of heat deposited in a unit mass of fluid) is given by cdT, where c is the fluid's specific heat per unit mass. However, the specific heat depends on what one holds fixed during the energy deposition: the fluid element's volume or its pressure. As we have assumed that the fluid motions are very slow, the fractional pressure fluctuations will be correspondingly small. (This does not preclude significant temperature fluctuations, provided they are compensated by density fluctuations of opposite sign. However, if there are temperature fluctuations, then these will tend to equalize through thermal conduction in such a way that the pressure does not change significantly.) Therefore, the relevant specific heat for a slowly moving fluid is the one at constant pressure, c_P, and we must write $Tds = c_P dT$.[1] Eq. (18.3c) then becomes a linear partial differential equation for the temperature

$$\boxed{\frac{dT}{dt} \equiv \frac{\partial T}{\partial t} + \mathbf{v} \cdot \boldsymbol{\nabla} T = \chi \nabla^2 T}\,, \tag{18.4}$$

where

$$\boxed{\chi = \kappa/\rho\, c_P} \tag{18.5}$$

is known as the *thermal diffusivity* and we have again taken the easiest route in treating c_P and ρ as constant. When the fluid moves so slowly that the advective term $\mathbf{v} \cdot \boldsymbol{\nabla} T$ is negligible, then Eq. (18.4) says that the heat simply diffuses through the fluid, with the thermal diffusivity χ being the diffusion coefficient for temperature.

The diffusive transport of heat by thermal conduction is similar to the diffusive transport of vorticity by viscous stress [Eq. (14.3)] and the thermal diffusivity χ is the direct analog of the kinematic viscosity ν. This motivates us to introduce a new dimensionless number known as the *Prandtl number*, which measures the relative importance of viscosity and heat conduction (in the sense of their relative abilities to produce a diffusion of vorticity and of heat):

$$\boxed{\mathrm{Pr} = \frac{\nu}{\chi}}\,. \tag{18.6}$$

For gases, both ν and χ are given to order of magnitude by the product of the mean molecular speed and the mean free path, and so Prandtl numbers are typically of order unity. (For air, $\mathrm{Pr} \sim 0.7$.) By contrast, in liquid metals the free electrons carry heat very efficiently compared with the transport of momentum (and vorticity) by diffusing ions, and so their Prandtl numbers are small. This is why liquid sodium is used as a coolant in nuclear power reactors. At the other end of the spectrum, water is a relatively poor thermal conductor

[1] See e.g. Turner (1973) for a more formal justification of the use of the specific heat at constant pressure rather than constant volume.

with Pr ~ 6, and Prandtl numbers for oils, which are quite viscous and poor conductors, measure in the thousands. Other Prandtl numbers are given in Table 18.1.

Fluid	ν (m^2s^{-1})	χ (m^2s^{-1})	Pr
Earth's mantle	10^{17}	10^{-6}	10^{23}
Solar interior	10^{-2}	10^{2}	10^{-4}
Atmosphere	10^{-5}	10^{-5}	1
Ocean	10^{-6}	10^{-7}	10

Table 18.1: Order of magnitude estimates for kinematic viscosity ν, thermal diffusivity χ, and Prandtl number $\mathrm{Pr} = \nu/\chi$ for earth, fire, air and water.

One might think that, when the Prandtl number is small (so κ is large compared to ν), one should necessarily include heat flow in the fluid equations and pay attention to thermally induced buoyancy (Sec. 18.3). Not so. In some low-Prandtl-number flows, the heat conduction is so effective that the fluid becomes essentially isothermal, and buoyancy effects are minimised. Conversely, in some large-Prandtl-number flows the large viscous stress reduces the velocity gradient so that slow, thermally driven circulation takes place and thermal effects are very important. In general, the kinematic viscosity is of direct importance in controlling the transport of momentum, and hence in establishing the velocity field, whereas heat conduction affects the velocity field only indirectly (Sec. 18.3 below). We must therefore examine each flow on its individual merits.

There is another dimensionless number that is commonly introduced when discussing thermal effects: the *Péclet number*. It is defined, by analogy with the Reynolds' number, by

$$\boxed{\mathrm{Pe} = \frac{LV}{\chi}}, \tag{18.7}$$

where L is a characteristic length scale of the flow and V is a characteristic speed. The Péclet number measures the relative importance of advection and heat conduction.

****

EXERCISES

Exercise 18.1 *Example: Poiseuille Flow with a uniform temperature gradient*
A nuclear reactor is cooled with liquid sodium which flows through a set of pipes from the reactor to a remote heat exchanger, where the heat's energy is used to generate electricity. Unfortunately, some heat will be lost through the walls of the pipe before it reaches the heat exchanger and this will reduce the reactor's efficiency. In this exercise, we determine what fraction of the heat is lost.

Consider the flow of the sodium through one of the pipes, and assume that the Reynold's number is modest so the flow is steady and laminar. Then the fluid velocity will have the parabolic Poiseuille profile

$$v = 2\bar{v}\left(1 - \frac{\varpi^2}{R^2}\right) \tag{18.8}$$

[Eq. (13.80) and associated discussion]. Here R is the pipe's inner radius, ϖ is the cylindrical radial coordinate measured from the axis of the pipe, and $\bar{v}$ is the mean speed along the pipe. Suppose that the pipe has length $L \gg R$ from the reactor to the heat exchanger, and is thermally very well insulated so its inner wall (at $\varpi = R$) is at nearly the same temperature as the core of the fluid (at $\varpi = 0$). Then the total temperature drop ΔT down the length L will be $\Delta T \ll T$, and the longitudinal temperature gradient will be constant, so the temperature distribution in the pipe has the form

$$T = T_0 - \Delta T \frac{z}{L} + f(\varpi) \ . \tag{18.9}$$

(a) Use Eq. (18.3c) to show that

$$f = \frac{\bar{v} R^2 \Delta T}{2\chi L} \left[\frac{3}{4} - \frac{\varpi^2}{R^2} + \frac{1}{4} \frac{\varpi^4}{R^4} \right] \ . \tag{18.10}$$

(b) Derive an expression for the conductive heat flux through the walls of the pipe and show that the ratio of the heat escaping through the walls to that advected by the fluid is $\Delta T/T$. (Ignore the influence of the temperature gradient on the velocity field and treat the thermal diffusivity and specific heat as constant throughout the flow.)

(c) Consider a nuclear reactor in which 10kW of power has to be transported through a pipe carrying liquid sodium. If the reactor temperature is $\sim$ 1000K and the exterior temperature is room temperature, estimate the flow of liquid sodium necessary to achieve the necessary transport of heat.

Exercise 18.2 *Problem: Thermal Boundary Layers*
In Sec. 14.4, we introduced the notion of a laminar boundary layer by analyzing flow past a thin plate. Now suppose that this same plate is maintained at a different temperature from the free flow. A thermal boundary layer will be formed, in addition to the viscous boundary layer, which we presume to be laminar. These two boundary layers will both extend outward from the wall but will (usually) have different thicknesses.

(a) Explain why their relative thicknesses depend on the Prandtl number.

(b) Using Eq. (18.4), show that in order of magnitude the thickness of the thermal boundary layer, δ_T, is given by

$$v(\delta_T)\delta_T^2 = \ell\chi \ ,$$

where $v(\delta_T)$ is the fluid velocity parallel to the plate at the outer edge of the thermal boundary layer and ℓ is the distance downstream from the leading edge.

(c) Let V be the free stream fluid velocity and ΔT be the temperature difference between the plate and the body of the flow. Estimate δ_T in the limits of large and small Prandtl numbers.

(d) What will be the boundary layer's temperature profile when the Prandtl number is exactly unity? [Hint: Seek a self similar solution to the relevant equations. For solution, see Sec. 31.1 of Lautrup (2005).]

****

18.3 T2 Boussinesq Approximation

When heat fluxes are sufficiently small, we can use Eq. (18.4) to solve for the temperature distribution in a given velocity field, ignoring the feedback of thermal effects onto the velocity. However, if we imagine increasing the flow's temperature differences so the heat fluxes also increase, at some point thermal feedback effects will begin to influence the velocity significantly. Typically, the first feedback effect to occur is *buoyancy*, the tendency of the hotter (and hence lower-density) fluid to rise in a gravitational field and the colder (and hence denser) fluid to descend.[2] In this section, we shall describe the effects of buoyancy as simply as possible. The minimal approach, which is adequate surprisingly often, is called the *Boussinesq approximation*. It can be used to describe many heat-driven laboratory flows and atmospheric flows, and some geophysical flows.

The types of flows for which the Boussinesq approximation is appropriate are those in which the fractional density changes are small ($|\Delta\rho| \ll \rho$). By contrast, the velocity can undergo large changes, though it remains constrained by the incompressibility relation (18.3a):

$$\boxed{\boldsymbol{\nabla}\cdot\mathbf{v} = 0\,. \quad \text{Boussinesq (1)}} \tag{18.11}$$

One might think that this implies the density is constant moving with a fluid element, since mass conservation says $d\rho/dt = -\rho\boldsymbol{\nabla}\cdot v$. However, thermal expansion causes small density changes, with tiny corresponding violations of Eq. (18.11); this explains the "$\simeq$" that we used in Eqs. (18.3a). The key point is that, for these types of flows, *the density is controlled to high accuracy by thermal expansion, and the velocity field is divergence free to high accuracy.*

In discussing thermal expansion, it is convenient to introduce a *reference density* ρ_0 and *reference temperature* T_0, equal to some mean of the density and temperature in the region of fluid that one is studying. We shall denote by

$$\boxed{\tau \equiv T - T_0} \tag{18.12}$$

the perturbation of the temperature away from its reference value. The thermally perturbed density can then be written as

$$\boxed{\rho = \rho_0(1 - \alpha\tau)}\,, \tag{18.13}$$

[2]This effect is put to good use in a domestic "gravity-fed" warm-air circulation system. The furnace generally resides in the basement not the attic!

where α is the thermal expansion coefficient for volume[3] [evaluated at constant pressure for the same reason as c_P was at constant pressure in the paragraph following Eq. (18.3c)]:

$$\boxed{\alpha = -\left(\frac{\partial \ln \rho}{\partial T}\right)_P} . \tag{18.14}$$

Equation (18.13) enables us to eliminate density perturbations as an explicit variable and replace them by temperature perturbations.

Turn, now, to the Navier-Stokes equation (18.3b) in a uniform external gravitational field. We expand the pressure-gradient term as

$$-\frac{\boldsymbol{\nabla} P}{\rho} \simeq -\frac{\boldsymbol{\nabla} P}{\rho_0}(1+\alpha\tau) \ , \tag{18.15}$$

and, as in our analysis of rotating flows [Eq. (14.55)], we introduce an *effective pressure* designed to compensate for the first-order effects of the uniform gravitational field:

$$\boxed{P' = P + \rho_0 \Phi = P - \rho_0 \boldsymbol{g}\cdot\mathbf{x}} . \tag{18.16}$$

(Notice that P' measures the amount the pressure differs from the value it would have in supporting a hydrostatic atmosphere of the fluid at the reference density.) The Navier-Stokes equation (18.3b) then becomes

$$\boxed{\frac{d\mathbf{v}}{dt} = -\frac{\boldsymbol{\nabla} P'}{\rho_0} - \alpha\tau\boldsymbol{g} + \nu\nabla^2\mathbf{v} \ , \quad \text{Boussinesq (2)}} \tag{18.17}$$

dropping the small term $O(\alpha P')$. In words, a fluid element accelerates in response to a buoyancy force which is the sum of the first and second terms on the right hand side of Eq. (18.17), and a viscous force.

In order to solve this equation, we must be able to solve for the temperature perturbation, τ. This evolves according to the standard equation of heat diffusion, Eq. (18.4):

$$\boxed{\frac{d\tau}{dt} = \chi\nabla^2\tau. \quad \text{Boussinesq (3)}} \tag{18.18}$$

Equations (18.11), (18.17) and (18.18) are the equations of fluid flow in the Boussinesq approximation; they control the coupled evolution of the velocity $\mathbf{v}$ and the temperature perturbation τ. We shall now use them to discuss free convection in a laboratory apparatus.

18.4 T2 Rayleigh-Bénard Convection – Mantle Convection and Continental Drift

In a relatively simple laboratory experiment to demonstrate convection, a fluid is confined between two rigid plates a distance d apart, each maintained at a fixed temperature, with

[3]Note that α is three times larger than the thermal expansion coefficient for the linear dimensions of the fluid.

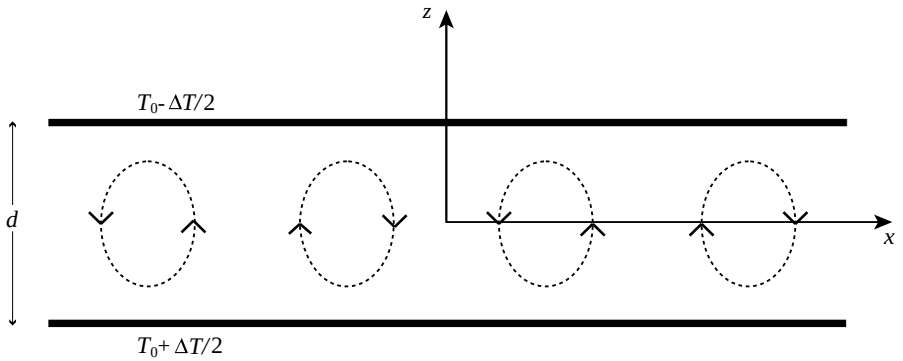

Fig. 18.1: Rayleigh-Bénard convection. A fluid is confined between two horizontal surfaces separated by a vertical distance d. When the temperature difference between the two plates ΔT is increased sufficiently, the fluid will start to convect heat vertically. The reference effective pressure P'_0 and reference temperature T_0 are the values of P' and T measured at the midplane $z = 0$.

the upper plate cooler than the lower by ΔT. When ΔT is small, viscous stresses, together with the no-slip boundary conditions at the plates, inhibit circulation; so, despite the upward buoyancy force on the hotter, less-dense fluid near the bottom plate, the fluid remains stably at rest with heat being conducted diffusively upward. If the plates' temperature difference ΔT is gradually increased, the buoyancy becomes gradually stronger. At some critical ΔT it will overcome the restraining viscous forces, and the fluid will start to circulate (convect) between the two plates. Our goal is to determine the critical temperature difference $\Delta T_{\rm crit}$ for the onset of convection.

We now make some physical arguments to simplify the calculation of $\Delta T_{\rm crit}$. From our experience with earlier instability calculations, especially those involving elastic bifurcations (Secs. 11.6.1 and 12.3.5), we anticipate that for $\Delta T < \Delta T_{\rm crit}$ the response of the equilibrium to small perturbations will be oscillatory (i.e., will have positive squared eigenfrequency ω^2), while for $\Delta T > \Delta T_{\rm crit}$, perturbations will grow exponentially (i.e., will have negative ω^2). Correspondingly, at $\Delta T = \Delta T_{\rm crit}$, ω^2 for some mode will be zero. This zero-frequency mode will mark the bifurcation of equilibria from one with no fluid motions to one with slow, convective motions. We shall search for $\Delta T_{\rm crit}$ by searching for a solution to the Boussinesq equations (18.11), (18.17) and (18.18) that represents this zero-frequency mode. In those equations we shall choose for the reference temperature T_0, density ρ_0 and effective pressure P_0 the values at the midplane between the plates, $z = 0$; cf. Fig. 18.1.

The unperturbed equilibrium, when $\Delta T = \Delta T_{\rm crit}$, is a solution of the Boussinesq equations (18.11), (18.17) and (18.18) with vanishing velocity, a time-independent vertical temperature gradient $dT/dz = -\Delta T/d$, and a compensating, time-independent, vertical pressure gradient:

$$\mathbf{v} = 0 \ , \quad \tau = T - T_0 = -\frac{\Delta T}{d} z \ , \quad P' = P'_0 + g\rho_0\alpha \frac{\Delta T}{d}\frac{z^2}{2} \ . \tag{18.19}$$

When the zero-frequency mode is present, the velocity $\mathbf{v}$ will be nonzero, and the temperature and effective pressure will have additional perturbations $\delta\tau$ and $\delta P'$:

$$\mathbf{v} \neq 0 \ , \quad \tau = T - T_0 = -\frac{\Delta T}{d} z + \delta\tau \ , \quad P' = P'_0 + g\rho_0\alpha \frac{\Delta T}{d}\frac{z^2}{2} + \delta P' \ . \tag{18.20}$$

The perturbations $\mathbf{v}$, $\delta\tau$ and $\delta P'$ are governed by the Boussinesq equations and the boundary conditions at the plates, $z = \pm d/2$, that $\mathbf{v} = 0$ (no-slip) and $\delta\tau = 0$. We shall manipulate these in such a way as to get a partial differential equation for the scalar temperature perturbation $\delta\tau$ by itself, decoupled from the velocity and the pressure perturbation.

Consider, first, the result of inserting expressions (18.20) into the Boussinesq-approximated Navier-Stokes equation (18.17). Because the perturbation mode has zero frequency, $\partial\mathbf{v}/\partial t$ vanishes; and because $\mathbf{v}$ is extremely small, we can neglect the quadratic advective term $\mathbf{v}\cdot\nabla\mathbf{v}$, thereby bringing Eq. (18.17) into the form

$$\frac{\boldsymbol{\nabla}\delta P'}{\rho_0} = \nu\nabla^2\mathbf{v} - \boldsymbol{g}\alpha\delta\tau \ . \tag{18.21}$$

We want to eliminate $\delta P'$ from this equation. The other Boussinesq equations are of no help for this, since $\delta P'$ is absent from them. One might be tempted to eliminate δP using the equation of state $P = P(\rho, T)$; but in the present analysis our Boussinesq approximation insists that the only significant changes of density are those due to thermal expansion, i.e. it neglects the influence of pressure on density, so the equation of state cannot help us. Lacking any other way to eliminate $\delta P'$, we employ a very common trick: we take the curl of Eq. (18.21). As the curl of a gradient vanishes, $\delta P'$ drops out. We then take the curl one more time and use the fact that $\boldsymbol{\nabla}\cdot\mathbf{v} = 0$ to obtain

$$\nu\nabla^2(\nabla^2\mathbf{v}) = \alpha\boldsymbol{g}\nabla^2\delta\tau - \alpha(\boldsymbol{g}\cdot\nabla)\nabla\delta\tau \ . \tag{18.22}$$

Turn, next, to the Boussinesq version of the equation of heat transport, Eq. (18.18). Inserting into it Eqs. (18.20) for τ and $\mathbf{v}$, setting $\partial\delta\tau/\partial t$ to zero because our perturbation has zero frequency, linearizing in the perturbation, and using $\boldsymbol{g} = -g\mathbf{e}_z$, we obtain

$$\frac{v_z\Delta T}{d} = -\chi\nabla^2\delta\tau \ . \tag{18.23}$$

This is an equation for the vertical velocity v_z in terms of the temperature perturbation $\delta\tau$. By inserting this v_z into the z component of Eq. (18.22), we achieve our goal of a scalar equation for $\delta\tau$ alone:

$$\boxed{\nu\chi\nabla^2\nabla^2\nabla^2\delta\tau = \frac{\alpha g\Delta T}{d}\left(\frac{\partial^2\delta\tau}{\partial x^2} + \frac{\partial^2\delta\tau}{\partial y^2}\right)} \ . \tag{18.24}$$

This is a sixth order differential equation, even more formidable than the fourth order equations that arise in the elasticity calculations of Chaps. 11 and 12. We now see how prudent it was to make simplifying assumptions at the outset!

The differential equation (18.24) is, however, linear, so we can seek solutions using separation of variables. As the equilibrium is unbounded horizontally, we look for a single horizontal Fourier component with some wave number k; i.e., we seek a solution of the form

$$\delta\tau \propto \exp(ikx) f(z) \ , \tag{18.25}$$

where $f(z)$ is some unknown function. Such a $\delta\tau$ will be accompanied by motions $\mathbf{v}$ in the x and z directions (i.e., $v_y = 0$) that also have the form $v_j \propto \exp(ikx) f_j(z)$ for some other functions $f_j(z)$.

The anszatz (18.25) converts the partial differential equation (18.24) into the single ordinary differential equation

$$\left(\frac{d^2}{dz^2} - k^2\right)^3 f + \frac{\mathrm{Ra}\, k^2 f}{d^4} = 0 \,, \tag{18.26}$$

where we have introduced yet another dimensionless number

$$\boxed{\mathrm{Ra} = \frac{\alpha g \Delta T d^3}{\nu\chi}} \tag{18.27}$$

called the *Rayleigh number*. By virtue of the relation (18.23) between v_z and $\delta\tau$, the Rayleigh number is a measure of the ratio of the strength of the buoyancy term $-\alpha\delta\tau\boldsymbol{g}$ to the viscous term $\nu\nabla^2\mathbf{v}$ in the Boussinesq version (18.17) of the Navier-Stokes equation:

$$\boxed{\mathrm{Ra} \sim \frac{\text{buoyancy force}}{\text{viscous force}}} \,. \tag{18.28}$$

The general solution of Eq. (18.26) is an arbitrary, linear combination of three sine functions and three cosine functions:

$$f = \sum_{n=1}^{3} A_n \cos(\mu_n k z) + B_n \sin(\mu_n k z) \,, \tag{18.29}$$

where the dimensionless numbers μ_n are given by

$$\mu_n = \left[\left(\frac{\mathrm{Ra}}{k^4 d^4}\right)^{1/3} e^{2\pi n i/3} - 1\right]^{1/2} \quad ; \quad n = 1, 2, 3 \,, \tag{18.30}$$

which involves the three cube roots of unity, $e^{2\pi n i/3}$. The values of five of the coefficients A_n, B_n are fixed in terms of the sixth (an overall arbitrary amplitude) by five boundary conditions at the bounding plates, and a sixth boundary condition then determines the critical temperature difference ΔT_{crit} (or equivalently, the critical Rayleigh number $\mathrm{Ra}_{\mathrm{crit}}$) at which convection sets in.

The six boundary conditions are: (i) The requirement that the fluid temperature be the same as the plate temperature at each plate, so $\delta\tau = 0$ at $z = \pm d/2$. (ii) The no-slip boundary condition $v_z = 0$ at each plate which, by virtue of Eq. (18.23) and $\delta\tau = 0$ at the plates, translates into $\delta\tau_{,zz} = 0$ at $z = \pm d/2$ (where the indices after the comma are partial derivatives). (iii) The no-slip boundary condition $v_x = 0$, which by virtue of incompressibility $\boldsymbol{\nabla}\cdot\mathbf{v} = 0$ implies $v_{z,z} = 0$ at the plates, which in turn by Eq. (18.23) implies $\delta\tau_{,zzz} + \delta\tau_{,xxz} = 0$ at $z = \pm d/2$.

It is straightforward but computationally complex to impose these six boundary conditions and from them deduce the critical Rayleigh number for onset of convection (Pellew and Southwell 1940). Rather than present the nasty details, we shall switch to a toy problem in which the boundary conditions are adjusted to give a simpler solution, but one with the

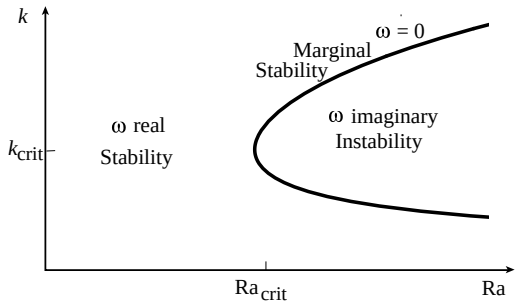

Fig. 18.2: Horizontal wave number k of the first mode to go unstable, as a function of Rayleigh number, Ra. Along the solid curve the mode has zero frequency; to the left of the curve it is stable, to the right it is unstable. $\mathrm{Ra}_{\mathrm{crit}}$ is the minimum Rayleigh number for convective instability.

same qualitative features as for the real problem. Specifically, we shall replace the no-slip condition (iii) ($v_x = 0$ at the plates) by a condition of no shear, (iii') $v_{x,z} = 0$ at the plates. By virtue of incompressibility $\boldsymbol{\nabla} \cdot \mathbf{v} = 0$, the x derivative of this translates into $v_{z,zz} = 0$, which by Eq. (18.23) translates to $\delta\tau_{,zzxx} + \delta\tau_{,zzzz} = 0$. To recapitulate, we seek a solution of the form (18.29), (18.30) that satisfies the boundary conditions (i), (ii), (iii').

The terms in Eq. (18.29) with $n = 1, 2$ always have complex arguments and thus always have z dependences that are products of hyperbolic and trigonometric functions with real arguments. For $n = 3$ and large enough Rayleigh number, μ_3 is positive and the solutions are pure sines and cosines. Let us just consider the $n = 3$ terms alone, in this regime, and impose boundary condition (i), that $\delta\tau = 0$ at the plates. The cosine term by itself,

$$\delta\tau = \text{constant} \times \cos(\mu_3 kz)\, e^{ikx} \ , \tag{18.31}$$

satisfies this, if we set

$$\frac{\mu_3 kd}{2} \equiv \left[\left(\frac{\mathrm{Ra}}{k^4 d^4}\right)^{1/3} - 1\right]^{1/2} \frac{kd}{2} = \left(m + \frac{1}{2}\right)\pi \ , \tag{18.32}$$

where m is an integer. It is straightforward to show, remarkably, that Eqs. (18.31), (18.32) also satisfy boundary conditions (ii) and (iii'), so they solve the toy version of our problem.

As ΔT is gradually increased from zero, the Rayleigh number Ra gradually grows, passing one after another through the sequence of values (18.32) with $m = 0, 1, 2, ...$ (for any chosen k). At each of these values there is a zero-frequency, circulatory mode of fluid motion with horizontal wave number k, which is passing from stability to instability. The first of these, $m = 0$, represents the onset of circulation for the chosen k, and the Rayleigh number at this onset [Eq. (18.32) with $m = 0$] is

$$\mathrm{Ra} = \frac{(k^2 d^2 + \pi^2)^3}{k^2 d^2} \ . \tag{18.33}$$

This $\mathrm{Ra}(k)$ relation is plotted as a thick curve in Fig. 18.2.

Notice in Fig. 18.2 that there is a critical Rayleigh number $\mathrm{Ra}_{\mathrm{crit}}$ below which all modes are stable, independent of their wave numbers, and above which modes in some range $k_{\min} <$

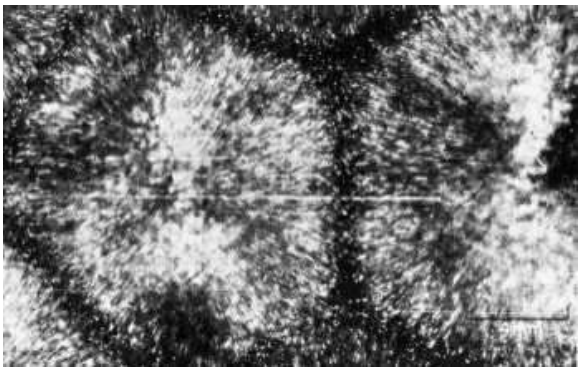

Fig. 18.3: Hexagonal convection cells in Rayleigh-Bénard convection. The fluid, which is visualized using aluminum powder, rises at the centers of the hexagons and falls around the edges.

$k < k_{\rm max}$ are unstable. From Eq. (18.33) we deduce that, for our toy problem, $\mathrm{Ra}_{\rm crit} = 27\pi^4/4 \simeq 660$.

When one imposes the correct boundary conditions (i), (ii), (iii) [instead of our toy choice (i), (ii), (iii')] and works through the nasty details of the computation, one obtains a $\mathrm{Ra}(k)$ relation that looks qualitatively the same as Fig. 18.2, and one deduces that convection should set in at $\mathrm{Ra}_{\rm crit} = 1708$, which agrees reasonably well with experiment. One can carry out the same computation with the fluid's upper surface free to move (e.g., due to placing air rather than a solid plate at $z = d/2$). Such a computation predicts that convection begins at $\mathrm{Ra}_{\rm crit} \simeq 1100$, though in practice surface tension is usually important and its effect must be included.

One feature of these critical Rayleigh numbers is very striking. Because the Rayleigh number is an estimate of the ratio of buoyancy forces to viscous forces [Eq. (18.28)], an order-of-magnitude analysis suggests that convection should set in at $\mathrm{Ra} \sim 1$—which is wrong by three orders of magnitude! This provides a vivid reminder that order-of-magnitude estimates can be quite inaccurate. In this case, the main reason for the discrepancy is that the convective onset is governed by a sixth-order differential equation (18.24), and thus is very sensitive to the lengthscale d used in the order-of-magnitude analysis. If we choose d/π rather than d as the length scale, then an order-of-magnitude estimate could give $\mathrm{Ra} \sim \pi^6 \sim 1000$, a much more satisfactory value.

Once convection has set in, the unstable modes grow until viscosity and nonlinearities stabilize them, at which point they carry far more heat upward between the plates than does conduction. The convection's velocity pattern depends, in practice, on the manner in which the heat is applied, the temperature dependence of the viscosity, and the fluid's boundaries. For a limited range of Rayleigh numbers near $\mathrm{Ra}_{\rm crit}$, it is possible to excite a hexagonal pattern of *convection cells* as shown in Fig. 18.3; but other patterns can also be excited.

Drazin and Reid (2004) suggest a kitchen experiment for observing convection cells: Place a 2 mm layer of corn or canola oil on the bottom of a skillet and sprinkle coco or Ovaltine or other powder over it. Heat the skillet bottom gently and uniformly. The motion of the powder particles will reveal the convection cells, with upwelling at the cell centers and surface powder collecting and falling at the edges.

In Rayleigh-Bernard convection experiments, as the Rayleigh number is increased beyond

the onset of convection, one or another sequences of equilibrium bifurcations leads to weak turbulence; see Sec. 15.6.3. When the Rayleigh number becomes very large, the convection becomes strongly turbulent.

Free convection, like that in these laboratory experiments, also occurs in meteorological and geophysical flows. For example for air in a room, the relevant parameter values are $\alpha = 1/T \sim 0.003$ K^{-1} (Charles' Law), and $\nu \sim \chi \sim 10^{-5}$ m^2 s^{-1}, so the Rayleigh number is $\mathrm{Ra} \sim 3 \times 10^8 (\Delta T/1\mathrm{K})(d/1\mathrm{m})^3$. Convection in a room thus occurs extremely readily, even for small temperature differences. In fact, so many modes of convective motion can be excited

Box 18.2
Mantle Convection and Continental Drift

As is now well known, the continents drift over the surface of the globe on a timescale of roughly a hundred million years. Despite the clear geographical evidence that the continents fit together, geophysicists were, for a long while, skeptical that this occurred because they were unable to identify the forces responsible for overcoming the visco-elastic resilience of the crust. It is now known that these motions are in fact slow convective circulation of the mantle driven by internally generated heat from the radioactive decay of unstable isotopes, principally uranium, thorium and potassium.

When the heat is generated within the convective layer (which has radial thickness d), rather than passively transported from below, we must modify our definition of the Rayleigh number. Let the heat generated per unit mass per unit time be Q. In the analog of our laboratory analysis, where the fluid is assumed marginally unstable to convective motions, this Q will generate a heat flux $\sim \rho Q d$, which must be carried diffusively. Equating this flux to $\kappa \Delta T/d$, we can solve for the temperature difference ΔT between the lower and upper edges of the convective mantle: $\Delta T \sim \rho Q d^2/\kappa$. Inserting this ΔT into Eq. (18.27), we obtain a modified expression for the Rayleigh number

$$\mathrm{Ra}' = \frac{\alpha \rho g Q d^5}{\kappa \chi \nu} \ . \tag{1}$$

Let us now estimate the value of Ra$'$ for the earth's mantle. The mantle's kinematic viscosity can be measured by post-glacial rebound studies (cf. Ex. 14.13) to be $\nu \sim 10^{17}$ m^2 s^{-1}. We can use the rate of attenuation of diurnal and annual temperature variation with depth in surface rock to estimate a thermal diffusivity $\chi \sim 10^{-6}$ m^2 s^{-1}. Direct experiment furnishes an expansion coefficient, $\alpha \sim 3 \times 10^{-5}$ K^{-1}. The thickness of the upper mantle is $d \sim 700$ km and the rock density is $\rho \sim 4000$ kg m^{-3}. The rate of heat generation can be estimated both by chemical analysis and direct measurement at the earth's surface and turns out to be $Q \sim 10^{-11}$ W kg^{-1}. Combining these quantities, we obtain an estimated Rayleigh number Ra$' \sim 10^6$, well in excess of the critical value for convection under free slip conditions which evaluates to $\mathrm{Ra}'_{\mathrm{crit}} = 868$ (Turcotte & Schubert 1982). For this reason, it is now believed that continental drift is driven primarily by mantle convection.

that heat-driven air flow is invariably turbulent. It is therefore common in everyday situations to describe heat transport using a phenomenological turbulent thermal conductivity (Sec. 15.4.2 of this book; Sec. 6.10.1 of White 2006).

A second example, convection in the Earth's mantle, is described in Box 18.2.

****

EXERCISES

Exercise 18.3 *Problem: Critical Rayleigh Number*
Estimate the temperature to which pans of oil ($\nu \sim 10^{-5}$ m^2 s^{-1}, Pr$\sim$ 3000), water ($\nu \sim 10^{-6}$ m^2 s^{-1}, Pr$\sim$ 6) and mercury ($\nu \sim 10^{-7}$ m^2 s^{-1}, Pr$\sim$ 0.02) would have to be heated in order to convect. Assume that the upper surface is at room temperature. Please don't perform this experiment with mercury.

Exercise 18.4 *Problem: Width of a Thermal Plume*
Consider a knife on its back, so its sharp edge points in the upward, z direction. The edge (idealized as extending infinitely far in the y direction) is hot, and by heating adjacent fluid it creates a rising thermal plume. Introduce a temperature deficit $\Delta T(z)$ that measures the typical difference in temperature between the plume and the surrounding, ambient fluid at height z above the knife edge, and let $\delta_p(z)$ be the width of the plume at height z.

(a) Show that energy conservation implies the constancy of $\delta_p \Delta T \bar{v}_z$, where $\bar{v}_z(z)$ is the plume's mean vertical speed at height z.

(b) Make an estimate of the buoyancy acceleration and use this to estimate $\bar{v}_z$.

(c) Use Eq. (18.18) to relate the width of the plume to the speed. Hence, show that the width of the plume scales as $\delta_p \propto z^{2/5}$ and the temperature deficit as $\Delta T \propto z^{-3/5}$.

(d) Repeat this exercise for a three dimensional plume above a hot spot.

****

18.5 Convection in Stars

The sun and other stars generate heat in their interiors by nuclear reactions. In most stars, the internal energy is predominantly in the form of hot hydrogen and helium ions and their electrons, while the thermal conductivity is due primarily to diffusing photons (Sec. 3.7), which have much longer mean free paths than the ions and electrons. When the photon mean free path becomes small due to high opacity (as happens in the outer 30 per cent of the sun; Fig. 18.4), the thermal conductivity goes down, so in order to transport the heat from nuclear burning, the star develops an increasingly steep temperature gradient. The star may then become convectively unstable and transport its energy far more efficiently by

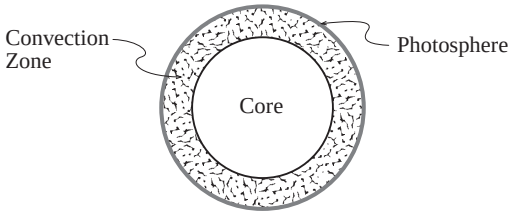

Fig. 18.4: A convection zone occupies the outer 30 per cent of a solar-type star.

circulating its hot gas than it could have by photon diffusion. Describing this convection is a key step in understanding the interiors of the sun and other stars.

A heuristic argument provides the basis for a surprisingly simple description of this convection. As a foundation for our argument, let us identify the relevant physics:

First: the pressure within stars varies through many orders of magnitude; a factor $\sim 10^{12}$ for the sun. Therefore, we cannot use the Boussinesq approximation; instead, as a fluid element rises or descends, we must allow for its density to change in response to large changes of the surrounding pressure. Second: The convection involves circulatory motions on such large scales that the attendant shears are small and viscosity is thus unimportant. Third: Because the convection is driven by the ineffectiveness of conduction, we can idealize each fluid element as retaining its heat as it moves, so the flow is adiabatic. Fourth: the convection will usually be very subsonic, as subsonic motions are easily sufficient to transport the nuclear-generated heat, except very close to the solar surface.

Our heuristic argument, then, focuses on convecting fluid blobs that move through the star's interior very subsonically, adiabatically, and without viscosity. As the motion is subsonic, each blob will remain in pressure equilibrium with its surroundings. Now, suppose

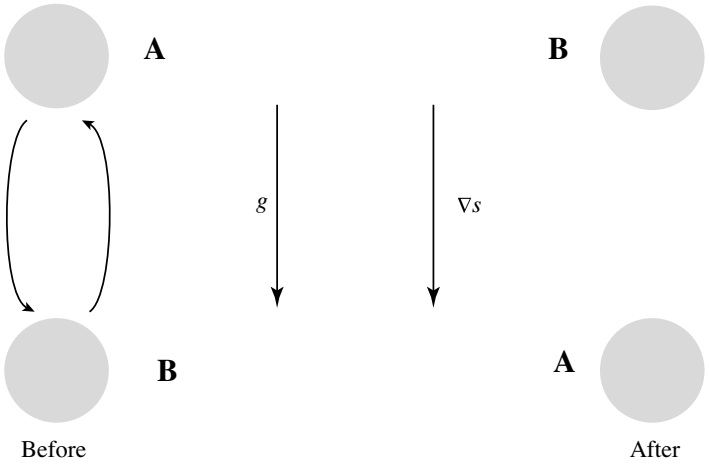

Fig. 18.5: Convectively unstable interchange of two blobs in a star whose entropy per unit mass increases downward. Blob B rises to the former position of blob A and expands adiabatically to match the surrounding pressure. The entropy per unit mass of the blob is higher than that of the surrounding gas and so the blob has a lower density. It will therefore be buoyant and continue to rise. Similarly, blob A will continue to sink.

we make a virtual interchange between two blobs at different heights (Fig. 18.5). The blob that rises (blob B in the figure) will experience a decreased pressure and thus will expand, so its density will diminish. If its density after rising is lower than that of its surroundings, then it will be buoyant and continue to rise. Conversely, if the risen blob is denser than its surroundings, then it will sink back to its original location. Therefore, a criterion for convective instability is that the risen blob has lower density than its surroundings. Since the blob and its surroundings have the same pressure, and since the larger is the entropy s per unit mass of gas, the lower is its density (there being more phase space available to its particles), the fluid is convectively unstable if the risen blob has a higher entropy than its surroundings. Now, the blob's motion was adiabatic, so its entropy per unit mass s is the same after it rises as before. Therefore, the fluid is convectively unstable if the entropy per unit mass s at the location where the blob began (lower in the star) is greater than that at the location to which it rose (higher in the star); i.e., *the star is convectively unstable if its entropy per unit mass decreases outward,* $ds/dr < 0$. For small blobs, this instability will be counteracted by both viscosity and heat conduction; but for large blobs, viscosity and conduction are ineffective, and the convection proceeds.

When building stellar models, astrophysicists find it convenient to determine whether a region of a model is convectively unstable by computing what its structure would be without convection, i.e., with all its heat carried radiatively. That computation gives some temperature gradient dT/dr. If this computed dT/dr is *superadiabiatic*, i.e., if

$$-\frac{d\ln T}{d\ln r} > \left(\frac{\partial \ln T}{\partial \ln P}\right)_s \left(-\frac{d\ln P}{d\ln r}\right) \equiv -\left(\frac{d\ln T}{d\ln r}\right)_s , \tag{18.34}$$

then correspondingly the entropy s decreases outward, and the star is convectively unstable. This is known as the *Schwarzschild criterion for convection*, since it was formulated by the same Karl Schwarzschild as discovered the Schwarzschild solution to Einstein's equations (which describes a nonrotating black hole; Chap. 26).

In practice, if the star is convective, then the convection is usually so efficient at transporting heat that the actual temperature gradient is only slightly superadiabatic; i.e., the entropy s is nearly independent of radius—it decreases outward only very slightly. (Of course, the entropy can *increase* significantly outwards in a convectively stable zone where radiative diffusion is adequate to transport heat.)

We can demonstrate the efficiency of convection by estimating the convective heat flux when the temperature gradient is slightly superadiabatic, i.e., when $\Delta|\boldsymbol{\nabla}T| \equiv |(dT/dr)| - |(dT/dr)_s|$ is slightly positive. As a tool in our estimate, we introduce the concept of the *mixing length*, denoted by l—the typical distance a blob travels before breaking up. As the blob is in pressure equilibrium, we can estimate its fractional density difference from its surroundings by $\Delta\rho/\rho \sim \Delta T/T \sim \Delta|\boldsymbol{\nabla}T|l/T$. Invoking Archimedes' principle, we estimate the blob's acceleration to be $\sim g\Delta\rho/\rho \sim g\Delta|\boldsymbol{\nabla}T|l/T$ (where g is the local acceleration of gravity), and hence the average speed with which a blob rises or sinks will be $\bar{v} \sim (g\Delta|\boldsymbol{\nabla}T|/T)^{1/2}l$. The convective heat flux is then given by

$$\begin{aligned} F_{\rm conv} &\sim c_P\rho\bar{v}l\Delta|\boldsymbol{\nabla}T| \\ &\sim c_P\rho(g/T)^{1/2}(\Delta|\boldsymbol{\nabla}T|)^{3/2}l^2 \ . \end{aligned} \tag{18.35}$$

We can bring this into a more useful form, accurate to within factors of order unity, by setting the mixing length equal to the pressure scale height $l \sim H = |dr/d\ln P|$ as is usually the case in the outer parts of a star, setting $c_P \sim h/T$ where h is the enthalpy per unit mass [cf. the first law of thermodynamics, Eq. (3) of Box 13.2], setting $g = -(P/\rho)d\ln P/dr \sim C^2|d\ln P/dr|$ [cf. the equation of hydrostatic equilibrium (13.13) and Eq. (16.48) for the speed of sound C], and setting $|\boldsymbol{\nabla} T| \equiv |dT/dr| \sim T d\ln P/dr$. The resulting expression for $F_{\rm conv}$ can then be inverted to give

$$\frac{|\Delta\boldsymbol{\nabla} T|}{|\boldsymbol{\nabla} T|} \sim \left(\frac{F_{\rm conv}}{h\rho C}\right)^{2/3} \sim \left(\frac{F_{\rm conv}}{\frac{5}{2}P\sqrt{k_B T/m_p}}\right)^{2/3} . \tag{18.36}$$

Here the last expression is obtained from the fact that the gas is fully ionized, so its enthalpy is $h = \frac{5}{2}P/\rho$ and its speed of sound is about the thermal speed of its protons (the most numerous massive particle), $C \sim \sqrt{k_B T/m_p}$ (with k_B Boltzmann's constant and m_p the proton rest mass).

It is informative to apply this estimate to the convection zone of the sun (the outer ~ 30 per cent of its radius; Fig. 18.4). The luminosity of the sun is $\sim 4\times 10^{26}$ W and its radius is 7×10^5 km, so its convective energy flux is $F_{\rm conv} \sim 10^8$ W m^{-2}. Consider, first, the convection zone's base. The pressure there is $P \sim 1$ TPa and the temperature is $T \sim 10^6$ K, so Eq. (18.36) predicts $|\Delta\boldsymbol{\nabla} T|/|\boldsymbol{\nabla} T| \sim 3\times 10^{-6}$; i.e., the temperature gradient at the base of the convection zone need only be superadiabatic by a few parts in a million in order to carry the solar energy flux.

By contrast, at the top of the convection zone (which is nearly at the solar surface), the gas pressure is only ~ 10 kPa and the sound speed is ~ 10 km s^{-1}, so $h\rho c \sim 10^8$W m^{-2}, and $|\Delta\boldsymbol{\nabla} T|/|\boldsymbol{\nabla} T| \sim 1$; i.e., the temperature gradient must depart significantly from the adiabatic gradient in order to carry the heat. Moreover, the convective elements, in their struggle to carry the heat, move with a significant fraction of the sound speed so it is no longer true that they are in pressure equilibrium with their surroundings. A more sophisticated theory of convection is therefore necessary near the solar surface.

Convection is very important in some other types of stars. It is the primary means of heat transport in the cores of stars with high mass and high luminosity, and throughout very young stars before they start to burn their hydrogen in nuclear reactions.

****

EXERCISES

Exercise 18.5 *Problem: Radiative Transport*
The density and temperature in the interior of the sun are roughly 0.1 kg m^{-3} and 1.5×10^7 K.

(a) Estimate the central gas pressure and radiation pressure and their ratio.

(b) The mean free path of the radiation is determined almost equally by Thomson scattering, bound-free absorption and free-free absorption. Estimate numerically the photon mean free path and hence estimate the photon escape time and the luminosity. How well do your estimates compare with the known values for the sun?

Exercise 18.6 *Problem: Bubbles*
Consider a small bubble of air rising slowly in a large expanse of water. If the bubble is large enough for surface tension to be ignored, then it will form an irregular cap of radius r. Show that the speed with which the bubble rises is roughly $\sim (gr)^{1/2}$. (A more refined estimate gives a numerical coefficient of 2/3.)

****

18.6 T2 Double Diffusion — Salt Fingers

Convection, as we have described it so far, is driven by the presence of an unbalanced buoyancy force in an equilibrium distribution of fluid. However, it can also arise as a higher order effect even if the fluid initially is stably stratified, i.e. if the density gradient is in the same direction as gravity. An example is *salt fingering*, a rapid mixing that can occur when warm, salty water lies at rest above colder fresh water. The higher temperature of the upper fluid outbalances the weight of its salt, making it more buoyant than the fresh water below. However, in a small, localized, downward perturbation of the warm, salty water, heat diffuses laterally into the colder surrounding water faster than salt diffuses, increasing the perturbation's density so it will continue to sink.

It is possible to describe this instability using a local perturbation analysis. The set up is somewhat similar to the one we used in Sec. 18.4 to analyze Rayleigh-Bénard convection: We consider a stratified fluid in an equilibrium state, in which there is a vertical gradient of the temperature, and as before, we measure its departure from a reference temperature T_0 at a midplane ($z = 0$) by $\tau \equiv T - T_0$. We presume that in the equilibrium state τ varies linearly with z, so $\boldsymbol{\nabla}\tau = (d\tau/dz)\mathbf{e}_z$ is constant. Similarly, we characterize the salt concentration by $\mathcal{C} \equiv$ (concentration) $-$ (equilibrium concentration at the mid plane); and we assume that in the equilibrium state, $\mathcal{C}$ like τ, varies linearly with height, so $\boldsymbol{\nabla}\mathcal{C} = (d\mathcal{C}/dz)\mathbf{e}_z$ is constant. The density ρ will be equal to the equilibrium density at the midplane plus corrections due to thermal expansion and due to salt concentration

$$\rho = \rho_0 - \alpha\rho_0\tau + \beta\rho_0\mathcal{C} \tag{18.37}$$

[cf. Eq. (18.13)]. Here β is a constant for concentration analogous to the thermal expansion coefficient α for temperature. In this problem, by contrast with Rayleigh-Bénard convection, it is easier to work directly with the pressure than the modified pressure. In equilibrium, hydrostatic equilibrium dictates that its gradient be $\boldsymbol{\nabla}P = -\rho\boldsymbol{g}$.

Now, let us perturb about this equilibrium state and write down the linearized equations for the evolution of the perturbations. We shall denote the perturbation of temperature (relative to the reference temperature) by $\delta\tau$, of salt concentration by $\delta\mathcal{C}$, of density by $\delta\rho$, of pressure by δP, and of velocity by simply $\mathbf{v}$ since the unperturbed state has $\mathbf{v} = 0$. We shall not ask about the onset of instability, but rather (because we expect our situation to be generically unstable) we shall seek a dispersion relation $\omega(\mathbf{k})$ for the perturbations. Correspondingly, in all our perturbation equations we shall replace $\partial/\partial t$ with $-i\omega$ and $\boldsymbol{\nabla}$ with $i\mathbf{k}$, except for the equilibrium $\boldsymbol{\nabla}\mathcal{C}$ and $\boldsymbol{\nabla}\tau$ which are constants.

The first of our perturbation equations is the linearized Navier-Stokes equation (18.3b)

$$-i\omega\rho_0\mathbf{v} = -i\mathbf{k}\delta P + \boldsymbol{g}\delta\rho - \nu k^2\rho_0\mathbf{v} \ , \tag{18.38a}$$

where we have kept the viscous term because we expect the Prandtl number to be of order unity (for water Pr ~ 6). Low velocity implies incompressibity $\boldsymbol{\nabla}\cdot\mathbf{v} = 0$, which becomes

$$\mathbf{k}\cdot\mathbf{v} = 0 \ . \tag{18.38b}$$

The density perturbation follows from the perturbed form of Eq. (18.37)

$$\delta\rho = -\alpha\rho_0\delta\tau + \beta\rho_0\delta\mathcal{C} \ . \tag{18.38c}$$

The temperature perturbation is governed by Eq. (18.18) which linearizes to

$$-i\omega\delta\tau + (\mathbf{v}\cdot\boldsymbol{\nabla})\tau = -\chi k^2\delta\tau \ . \tag{18.38d}$$

Assuming that the timescale for the salt to diffuse is much longer than that for the temperature to diffuse, we can ignore salt diffusion altogether so that $d\delta\mathcal{C}/dt = 0$, which becomes

$$-i\omega\delta\mathcal{C} + (\mathbf{v}\cdot\boldsymbol{\nabla})\mathcal{C} = 0 \ . \tag{18.38e}$$

Equations (18.38) are five equations for the five unknowns $\delta P, \delta\rho, \delta\mathcal{C}, \delta\tau, \mathbf{v}$, one of which is a three component vector! Unless we are careful, we will end up with a seventh order algebraic equation. Fortunately, there is a way to keep the algebra manageable. First, we eliminate the pressure perturbation by taking the curl of Eq. (18.38a) [or equivalently by crossing $\mathbf{k}$ into Eq. (18.38a)]:

$$(-i\omega + \nu k^2)\rho_0\mathbf{k}\times\mathbf{v} = \mathbf{k}\times\boldsymbol{g}\delta\rho \ . \tag{18.39a}$$

Taking the curl of this equation again allows us to incorporate incompressibility (18.38b):

$$(i\omega - \nu k^2)\rho_0 k^2\boldsymbol{g}\cdot\mathbf{v} = [(\mathbf{k}\cdot\boldsymbol{g})^2 - k^2g^2]\delta\rho \ . \tag{18.39b}$$

Since $\boldsymbol{g}$ points vertically, this is one equation for the density perturbation in terms of the vertical velocity perturbation v_z. We can obtain a second equation of this sort by inserting Eq. (18.38d) for $\delta\tau$ and Eq. (18.38e) for $\delta\mathcal{C}$ into Eq. (18.38c); the result is

$$\delta\rho = -\left(\frac{\alpha\rho_0}{i\omega - \chi k^2}\right)(\mathbf{v}\cdot\boldsymbol{\nabla})\tau + \frac{\beta\rho_0}{i\omega}(\mathbf{v}\cdot\boldsymbol{\nabla})\mathcal{C} \ . \tag{18.39c}$$

Since the unperturbed gradients of temperature and salt concentration are both vertical, Eq. (18.39c), like (18.39b), involves only v_z and not v_x or v_y. Solving both (18.39b) and (18.39c) for the ratio $\delta\rho/v_z$ and equating these two expressions, we obtain the following dispersion relation for our perturbations:

$$\omega(\omega + i\nu k^2)(\omega + i\chi k^2) + \left[1 - \frac{(\mathbf{k}\cdot\boldsymbol{g})^2}{k^2g^2}\right][\omega\alpha(\boldsymbol{g}\cdot\nabla)\tau - (\omega + i\chi k^2)\beta(\boldsymbol{g}\cdot\nabla)\mathcal{C}] = 0 \ . \tag{18.40}$$

When $\mathbf{k}$ is real, as we shall assume, we can write this dispersion relation as a cubic equation for $p = -i\omega$ with real coefficients. The roots for p are either all real or one real and two complex conjugates, and growing modes have the real part of p positive. When the constant term in the cubic is negative, i.e. when

$$(\boldsymbol{g} \cdot \nabla)\mathcal{C} < 0 \ , \tag{18.41}$$

we are guaranteed that there will be at least one positive, real root p and this root will correspond to an unstable, growing mode. Therefore, *a sufficient condition for instability is that the concentration of salt increase with height!*

By inspecting the dispersion relation we conclude that the growth rate will be maximal when $\mathbf{k} \cdot \boldsymbol{g} = 0$, i.e. when the wave vector is horizontal. What is the direction of the velocity $\mathbf{v}$ for these fastest growing modes? Incompressibility (18.38b) says that $\mathbf{v}$ is orthogonal to the horizontal $\mathbf{k}$; and Eq. (18.39a) says that $\mathbf{k} \times \mathbf{v}$ points in the same direction as $\mathbf{k} \times \boldsymbol{g}$, which is horizontal since $\boldsymbol{g}$ is vertical. These two conditions imply that $\mathbf{v}$ points vertically. Therefore, these fastest modes represent *fingers* of salty water descending past rising fingers of fresh water; cf. Fig. 18.6. For large k (narrow fingers), the dispersion relation (18.40) predicts a growth rate given approximately by

$$p = -i\omega \sim \frac{\beta(-\boldsymbol{g} \cdot \boldsymbol{\nabla})\mathcal{C}}{\nu k^2} \ . \tag{18.42}$$

Thus, the growth of narrow fingers is driven by the concentration gradient and retarded by viscosity. For larger fingers, the temperature gradient will participate in the retardation, since the heat must diffuse in order to break the buoyant stability.

Now let us turn to the nonlinear development of this instability. Although we have just considered a single Fourier mode, the fingers that grow are roughly cylindrical rather than sheet-like. They lengthen at a rate that is slow enough for the heat to diffuse horizontally, though not so slow that the salt can diffuse. Let the diffusion coefficient for the salt be $\chi_{\mathcal{C}}$ by analogy with χ for temperature. If the length of the fingers is L and their width is δ_f,

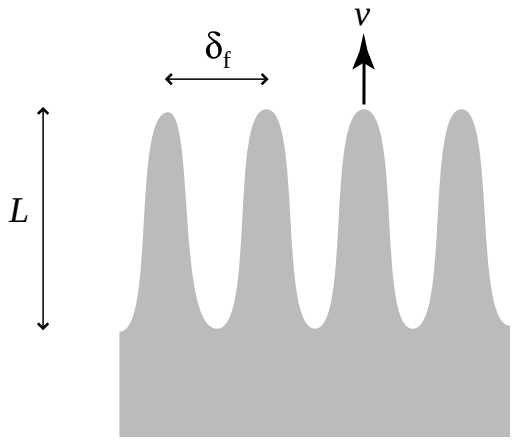

Fig. 18.6: Salt fingers in a fluid in which warm, salty water lies on top of cold fresh water.

then to facilitate heat diffusion and prevent salt diffusion, the vertical speed v must satisfy

$$\frac{\chi_{\mathcal{C}}\, L}{\delta_f^2} \ll v \ll \frac{\chi\, L}{\delta_f^2}\ . \tag{18.43}$$

Balancing the viscous acceleration $v\nu/\delta_f^2$ by the buoyancy acceleration $g\beta\delta\mathcal{C}$, we obtain

$$v \sim \frac{g\beta\delta\mathcal{C}\delta_f^2}{\nu}\ . \tag{18.44}$$

We can therefore re-write Eq. (18.43) as

$$\left(\frac{\chi_{\mathcal{C}}\nu L}{g\beta\delta\mathcal{C}}\right)^{1/4} \ll \delta_f \ll \left(\frac{\chi\nu L}{g\beta\delta\mathcal{C}}\right)^{1/4}\ . \tag{18.45}$$

Typically, $\chi_{\mathcal{C}} \sim 0.01\chi$, so Eq. (18.45) implies that the widths of the fingers lie in a narrow range, as is verified in laboratory experiments.

Salt fingering can occur naturally, for example in an estuary where cold river water flows beneath sea water warmed by the sun. However, the development of salt fingers is quite slow and in practice it only leads to mixing when the equilibrium velocity field is very small.

This instability is one example of a quite general type of instability known as *double diffusion* which can arise when two physical quantities can diffuse through a fluid at different rates. Other examples include the diffusion of two different solutes and the diffusion of vorticity and heat in a rotating flow.

****

EXERCISES

Exercise 18.7 *Problem: Laboratory experiment*
Make an order of magnitude estimate of the size of the fingers and the time it takes for them to grow in a small transparent jar. You might like to try an experiment.

Exercise 18.8 *Problem: Internal Waves*
Consider a stably stratified fluid at rest and let there be a small (negative) vertical density gradient, $d\rho/dz$.

(a) By modifying the above analysis, ignoring the effects of viscosity, heat conduction and concentration gradients, show that small-amplitude linear waves, which propagate in a direction making an angle θ to the vertical, have an angular frequency given by $\omega = N|\sin\theta|$, where $N \equiv [(\mathbf{g}\cdot\nabla)\ln\rho]^{1/2}$ is known as the *Brunt-Väisälä frequency*. These waves are called *internal waves*. (We have met another type of internal wave in Sec. 14.6.1, one supported by a stratified horizontal velocity distribution. For elastic materials such as the earth's crust, the analog of an internal fluid wave is an *edge wave*; see beginning of Sec. 12.4.2.)

(b) Show that the group velocity of these waves is orthogonal to the phase velocity and interpret this result physically.

****

Box 18.3
Important Concepts in Chapter 18

- Thermal conductivity, κ, and diffusive heat conduction, Sec. 18.2
- Thermal diffusivity, $\chi = \kappa/\rho c_P$, and diffusion equation for temperature, Sec. 18.2
- Thermal expansion coefficient, $\alpha = (\partial \ln \rho/\partial T)_P$, Sec. 18.3
- Prandtl number, Pr= ν/χ ∼(vorticity diffusion)/(heat diffusion), Sec. 18.2
- Péclet number, Pe= VL/χ ∼(advection)/(conduction), Sec. 18.2
- Rayleigh number Ra=$\alpha g/\Delta T d^3/(\nu\chi)$ ∼(buoyancy)/(viscous force), Sec. 18.4
- Boussinesq approximation for analyzing thermally induced buoyancy, Sec. 18.3
- Free convection and forced convection, Sec. 18.1
- Rayleigh-Bénard (free) convection, Sec. 18.4 and Fig. 18.1
- Critical Rayleigh number for onset of Rayleigh-Bénard convection, Sec. 18.4
- Schwarzschild criterion for convection in stars, Sec. 18.5
- Double-diffusion instability, Sec. 18.6

Bibliographic Note

For pedagogical treatments of almost all the topics in this chapter plus much more related material, we particuarly like Tritton (1988), whose phenomenological approach is lucid and appealing; and also Turner (1973), which is a thorough treatise on the influence of buoyancy (thermally induced and otherwise) on fluid motions.

Lautrup (2005) treats very nicely all this chapter's topics except convection in stars, salt fingers and double diffusion. In their Chaps. 5 and 6, Landau and Lifshitz (1959) give a fairly succinct treatment of diffusive heat flow in fluids, the onset of convection in several different physical situations, and the concepts underlying double diffusion. In his Chaps. 2–6, Chandrasekhar (1961) gives a thorough and rich treatment of the influence of a wide variety of phenomena on the onset of convection, and on the types of fluid motions that can occur near the onset of convection. For a few pages on strongly turbulent convective heat transfer, see Sec. 6-10 of White (2004).

Engineering oriented textbooks typically say little about convection. For an engineer's viewpoint and engineering issues in convection, we recommend more specialized texts such as Bejan (2013). For an applied mathematician's viewpoint, we suggest the treatise by Pop and Ingham (2001).

Bibliography

Bejan, Adrian 2013. *Convection Heat Transfer*, fourth edition, New York: Wiley

Chandrasekhar, S. 1961. *Hydrodynamics and Hydromagnetic Stability*, Oxford: Oxford University Press.

Drazin, P. G. and Reid, W. H. 2004. *Hydrodynamic Stability*, second edition, Cambridge: Cambridge University Press

Landau, L. D. and Lifshitz, E. M. 1959. *Fluid Dynamics*, Oxford: Pergamon.

Lautrup, B. 2005. *Physics of Continuous Matter*, Bristol UK: Institute of Physics.

Pellew, A. and Southwell, R. V. 1940. "On Maintained Convective Motion in a Fluid Heated from Below", *Proceedings of the Royal Society* **A176**, 312–343.

Pop, I. and Ingham, Derek B. 2001. *Convective Heat Transfer: Mathematical ad Computational Modelling of Viscous Fluids and Porous Media*, Amsterdam: Elsevier

Tritton, D. J. 1988. *Physical Fluid Dynamics*, second edition, Oxford: Oxford University Press.

Turcotte, D. L. and Schubert, G. 1982. *Geodynamics*, New York: Wiley.

Turner, J. S. 1973. *Buoyancy Effects in Fluids*, Cambridge: Cambridge University Press.

White, Frank M. 2004. *Viscous Fluid Flow*, third edition, New York: McGraw-Hill.